



This open access document is published as a preprint in the Beilstein Archives with doi: 10.3762/bxiv.2019.107.v1 and is considered to be an early communication for feedback before peer review. Before citing this document, please check if a final, peer-reviewed version has been published in the Beilstein Journal of Nanotechnology.

This document is not formatted, has not undergone copyediting or typesetting, and may contain errors, unsubstantiated scientific claims or preliminary data.

Preprint Title Flexible nanocellulose-based aerogel with loading of modified UiO-66 as efficient adsorbent for removal of heavy metal ions

Authors Jiajia Li, Sicong Tan, Nannan Rong, Kunjie Zhang, Mengting Xu and Zhaoyang Xu

Publication Date 17 Sep 2019

Article Type Full Research Paper

ORCID® IDs Zhaoyang Xu - <https://orcid.org/0000-0002-4118-7639>

Flexible nanocellulose-based aerogel with loading of modified UiO-66 as efficient adsorbent for removal of heavy metal ions

Jiajia Li¹, Sicong Tan¹, Nannan Rong¹, Kunjie Zhang¹, Mengting Xu¹, Zhaoyang Xu^{*1,2}

¹College of Materials Science and Engineering, Nanjing Forestry University, Nanjing 210037, China

²Key Laboratory of Bio-based Material Science & Technology, Northeast Forestry University, Haerbin 150040, China

*Corresponding author: Zhaoyang Xu (✉) Telephone and fax: +86-2585427517

E-mail: zhaoyangxunjfu@hotmail.com

Abstract

Currently, preparation of outstanding adsorbents has attracted public concern in environmentally friendly and sustainable pollutant redress. Herein, we report a directional freeze-drying method to prepare a flexible and reusable adsorbent through introducing modified metal-organic framework material (UiO-66-EDTA) into cellulose nanofibers (CNF) aerogel. By controlling the concentration of crosslinkable carboxymethyl cellulose (CMC) solution, we produced aerogels with different pore structures, fibrillar, columnar and lamellar morphology. The obtained UiO-66-EDTA/CNF/CMC aerogel (U-EDTA/CCA) showed excellent adsorption performance for total 9 types of heavy metal ions with the removal efficiency reaching 91%. Moreover, the aerogels could retain 88% of its original shape after 5 times cycling. The aerogel may be appropriate material for adsorbing heavy metal ions.

Keywords: nanocellulose aerogel, metal-organic framework, heavy metal ions, adsorption, directional freeze-drying.

Introduction

Sewage disposal is a global concern subject due to the destructive effect on ecologic sustainability. Wastewater, produced during the industrial manufacture such as textiles, cosmetics and chemical plant, contains many types of toxic dyes, oil and heavy metal ions[1-3]. To address this issue, various technologies have been researched and developed to dispose heavy metal ions within aqueous solution, such as membrane filtration[4], chemical coagulation[5], ions exchange[6], electrochemistry deposition[7, 8], and adsorption[9, 10]. Amongst above methods, adsorption, is the most feasible way due to its simple preparation, cost-effective and outstanding efficiency [11-14] and has attracted worldwide attention. Thus, various adsorbents have been developed to purify heavy metal ions from aqueous solution.

Aerogel, as a new generation of 3D network material, possesses many applications such as catalyze[15], adsorption [16, 17], and energy storage equipment [18, 19] due to its various superior properties including high porosity, low cost and large specific surface area. However, poor mechanical properties often impede the practical application of aerogels as adsorbents. Thus, many researches have been reported to improve this situation. For instance, Wu et al. added CNF into aerogels, hoping to enhance the mechanical strength of the hybrid material[20]. Not merely as a reinforcer, CNF can also be used as template for aerogels [10, 21]. To compare with other sorts of aerogels, CNF aerogels not only possesses high porosity and large surface

area, but also own high flexibility and strong mechanical property [22, 23]. Usually, freeze-drying or supercritical CO₂ drying method are used to fabricate porosity and flexibility CNF aerogels [15, 24]. Nevertheless, pure CNF tends to re-disperse in water which results in poor reusability. In order to overcome this problem, many technologies have been developed to strengthen the mechanical properties of CNF aerogels [25-27]. For example, Xu et al. prepared hydrophobic CNF/PVA aerogels modified via chemical vapor deposition which kept a stable structure in water [28]. Introducing extra adsorbing materials may also be an effective way to address this issue.

Metal-organic frameworks (MOFs), as a new generation porosity material, are built from organic ligands and metal nodes, with tunable pore structure, large surface areas and have attracted much research attention in different application fields [29-32]. MOFs have been demonstrated to play a crucial part when purifying wastewater containing heavy metal ions and other different industrial waste dyes [3, 33]. Lately, MOF-808 adsorbent grafted by EDTA showed great adsorption performance and high removal efficiency (>99%) was produced by Peng et al [34]. Because of the natural crystalline property of MOFs, which are commonly formed in powder form with nano-scale, made them hard to recycle [35, 36]. Introducing MOFs into CNF aerogel may not only take advantage of the stable mechanical structure of CNF but also maintain the huge surface area and high porosity of MOFs.

Herein, we report a simple technology to prepare an excellent adsorbent for removing heavy metal ions, through combining modified MOFs (UiO-66-EDTA) with CNF aerogels followed by directional freeze-drying. The aerogels possessed different

pore structures like fibrous, cylindrical, or lamellar morphologies and showed both outstanding mechanical properties and high removal efficiency. Moreover, the U-EDTA_{CCA} showed high stability for no obvious deformation was observed after several times cycling. The prepared aerogels showed great potential in practical applications for removing heavy metal ions.

Results and discussion

Preparation of U-EDTA_{CCA}

The preparation procedure of the U-EDTA_{CCA} is shown in Figure 1 and Figure 2. The excellent adsorbent was formed by loading functional UiO-66-EDTA into nanocellulose aerogels network. Figure 2 shows the schematic illustration of directional freeze-drying. The anisotropic U-EDTA_{CCAs} were fabricated via directional freeze-drying which could make aerogels form tunable pore structure (Figure 2D). By using this method, water would be rapidly frozen into ice crystals and grow vertically in the horizontal direction. Through controlling the concentration of CMC, aerogels with fibrous, cylindrical and lamellar structure were produced.



Figure 1: Experimental process of the UiO-66-EDTA-containing CNF suspension.

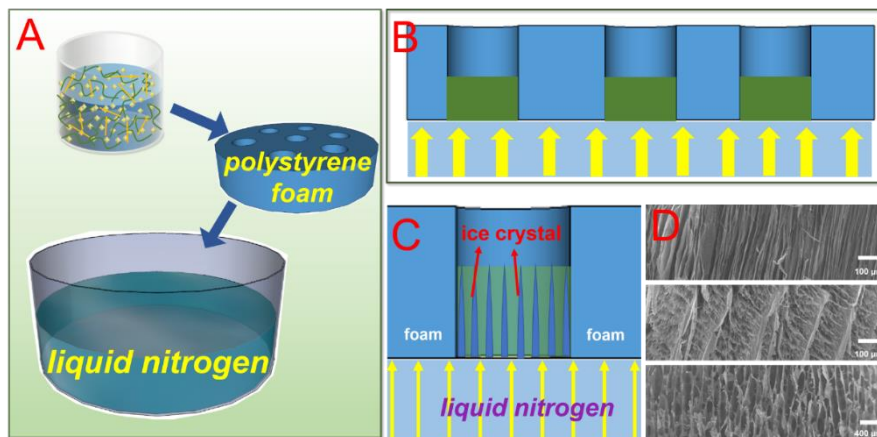


Figure 2: A, B, C) Experimental process of the directional freeze-drying. D) Morphology of the U-EDTA CCA via directional freeze-drying.

Surface morphology analysis

Surface morphology and the alignment degree of U-EDTA CCA was examined by SEM. Figure 3A, D and G shows the direction of the ice-growth which exhibits three general trends. First, 1wt% CMC solution was added in precursor U-EDTA/CNF solution and the aerogels showed a fibrous structure (Figure 3D-F). Then, the fibrillar structure turned into a cylindrical structure as the CMC solution was increased to 2 wt% (Figure 3A-B). Lastly, at the concentration of 4 wt%, the morphology of the aerogels turned into a lamellar form (Figure 3G-H). Figure 3B and E shows the top view of the U-EDTA CCA. The Figure 3C and I exhibited that UiO-66-EDTA nanoparticle was loaded on the lamina of the aerogels. In general, UiO-66-EDTA particles were dispersed among the aerogel pore walls and no particle agglomerate were observed (Figure 3 C and D). It may be concluded that anisotropic pore structure aerogels loaded with MOFs particles were successfully fabricated via directional freeze-casting. This anisotropic pore structure could enhance the mechanical properties of aerogels and increase adsorption rate.

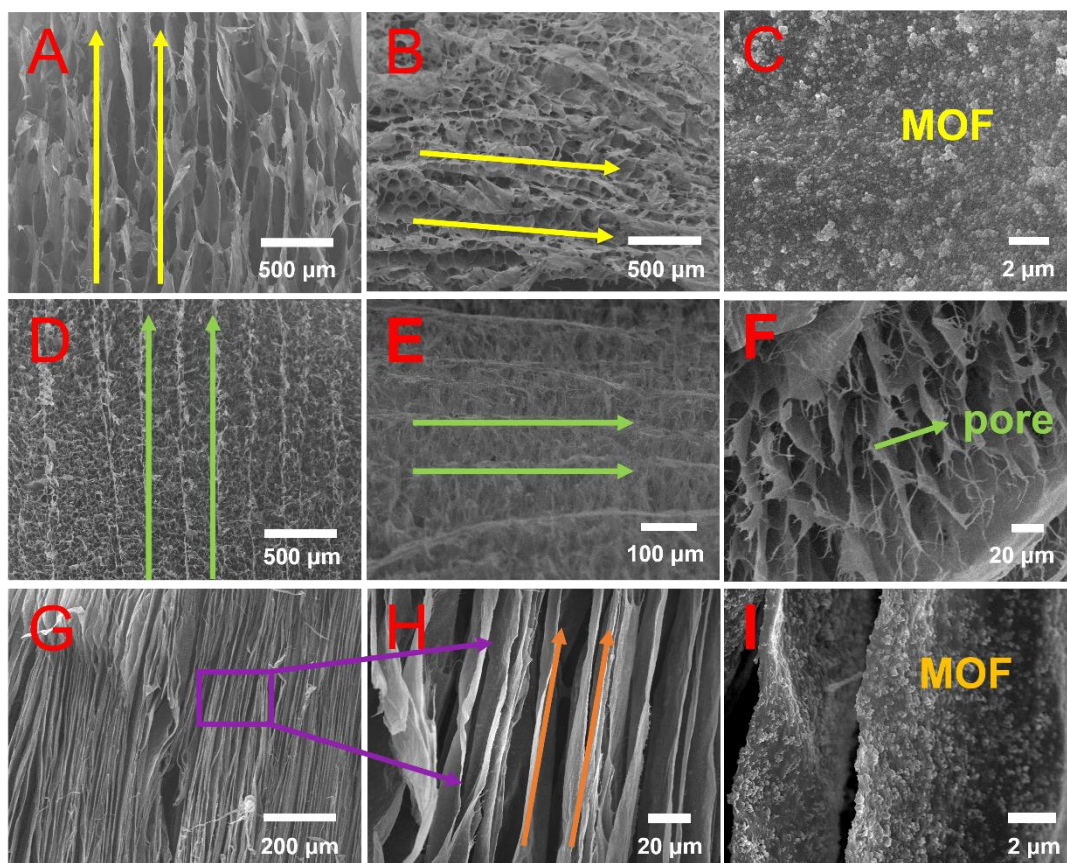


Figure 3: Morphology analysis of U-EDTA CCA. A, D, G) Show images of the ice-growth direction. B, E) Show the top view of the U-EDTA CCA prepared by directional freeze-casting method. C, I) Exhibit MOF particles loaded on the laminae of aerogels.

Chemical composition

The prominent performance of U-EDTA CCA as adsorbent derived from the tough chelation between metal ions and EDTA were measured by XPS. In this part, Ni^{2+} , Co^{2+} and Mn^{2+} were selected as testing examples. As shown in Figure 4A to Figure 4C, the wide-scan XPS spectra showed that metal ions were adsorbed in the pores of U-EDTA CCA. Core levels located at 855.3, 783.1 and 643.4 eV were caused by Ni^{2+} , Co^{2+} and Mn^{2+} respectively. Furthermore, Figure 4D showed XRD patterns of the prepared samples. The two characteristic peaks located at 7.4° and 8.5° were corresponded to

(111) and (002) planes of UiO-66 respectively, which demonstrated that the crystallinity was well preserved. The intensity of these peaks could be controlled by the amount of BDC to $ZrCl_4$. Compared the three materials' diffraction peaks, U-EDTACCA and UiO-66-EDTA were similarly to the UiO-66, indicating that UiO-66-EDTA was grown on hybrid aerogels surface successfully. The IR measurement was also used to evidence the existence of the introduced functional groups on the linkers for all the samples. In Figure 4E, peaks centered at about 1656, 1582, 1507 and 1395 cm^{-1} were caused by the stretching vibration of C=O in the carboxylic acid, the typical vibration of C=C in a benzene ring and O–C–O symmetric and asymmetric stretching in the BDC ligand, respectively. The FTIR spectrum of hybrid aerogel was shown in Fig. 4F and the several wide absorption peaks 3334, 2901, and 1031 cm^{-1} were caused by –OH, C–H and C–O–C stretching vibrations respectively. The peak ranged from 1110 to 1164 cm^{-1} might be the asymmetric tensile vibration of the glycosidic ring. In addition, the FTIR spectra of UiO-66-EDTA showed that the newly showed peak centered at 1300–1190 cm^{-1} could be caused by the C–N stretching band.

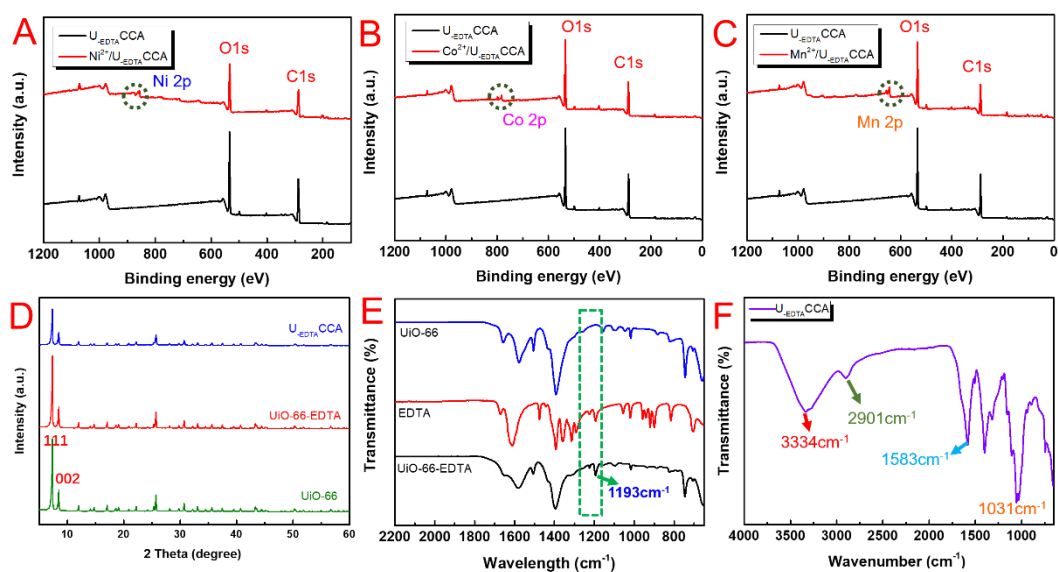


Figure 4: A-C) Comparison of wide-scan XPS spectra of U-EDTA CCA loading and un-loading Ni²⁺, Co²⁺ and Mn²⁺, respectively. D) XRD diffraction spectra of UiO-66, UiO-66-EDTA and U-EDTA CCA. E) The IR spectra of UiO-66, EDTA and UiO-66-EDTA. F) The IR spectra of U-EDTA CCA.

Adsorption performance analysis

In this paper, we selected total 9 kinds target metal ions to evaluate the efficiency of U-EDTA CCA as adsorbent. U-EDTA CCA was added into 10 ml aqueous solution containing heavy metal ions with a concentration of 10 mg/L under the condition of pH= 5. In Figure 5A, B, C, the kinetic behavior was studied by testing U-EDTA CCAs adsorption capacities (Q_t) at different time. In Figure 5D, U-EDTA CCA showed outstanding removal efficiency (>91%) for all the measured metal ions and this result was much higher than pure CNF aerogels. Apparently, the excellent adsorption ability for heavy metal ions of U-EDTA CCA was attributed to the powerful chelating between target ions and EDTA in hybrid aerogels. The special property of the prepared aerogels made it versatile in adsorbing several kinds of metal ions. In Figure 5E, 5 kinds of metal ions were captured with high removal efficiency (>91%). This result indicated that U-EDTA CCA was a potential material for purifying wastewater containing various metal ions. Moreover, the adsorption capacities of U-EDTA CCA showed a clear advantage for versatile heavy metal ions compared to other adsorbent (Table 1.). Above all, Large pores at micron level and the anisotropy pore structure of CNF aerogels were benefit for the fast removal of heavy metal ions and promoted the contact between functional UiO-66-EDTA particles and heavy metal ions.

Heavy metal ion-loaded U-EDTACCA aerogels were further measured via elemental mapping using SEM. In Figure 6A, elemental mapping indicated that zirconium was well-dispersed within U-EDTACCA, which could be used as particular metal connected sites for the command of metal ions' dispersion in aerogel adsorbents. Figure 6B-E showed the elemental mappings of specific metal ions-loaded U-EDTACCA. It was shown that Cr³⁺, Ni²⁺, Co²⁺ and Mn²⁺ were uniformly dispersed in the aerogels which gave good prove of our hypothesis.

Table 1: Comparison of the adsorption of metal ions of U-EDTACCA with other adsorbents.

adsorbents	Q _{max} (mg g ⁻¹)								reference
	Cu ²⁺	Cr ³⁺	Co ²⁺	Ni ²⁺	Mn ²⁺	Zn ²⁺	Fe ³⁺	Zr ⁴⁺	
UiO-66-NH ₂ @CA	39.33								[37]
^a Am-WS		135.7							[12]
^b 2C- g- PAN			100.18	49.29					[14]
^c 3CMC- g- PAA/MT						286.67			[38]
^d 4Phos-CNCSL							115		[39]
carboxymethylated cellulose fiber	16.90			11.63					[40]
Activated carbon					172				[41]
U-EDTACCA	137	396.	307	101	251	215	115	165	This work

^aAmidoximated wood sawdust

^bcellulose - graft - polyacrylonitrile

^ccarboxymethyl cellulose - graft - poly (acrylic acid)/ monmorilonite
^dphosphorylated cellulose nanocrystals from sludge

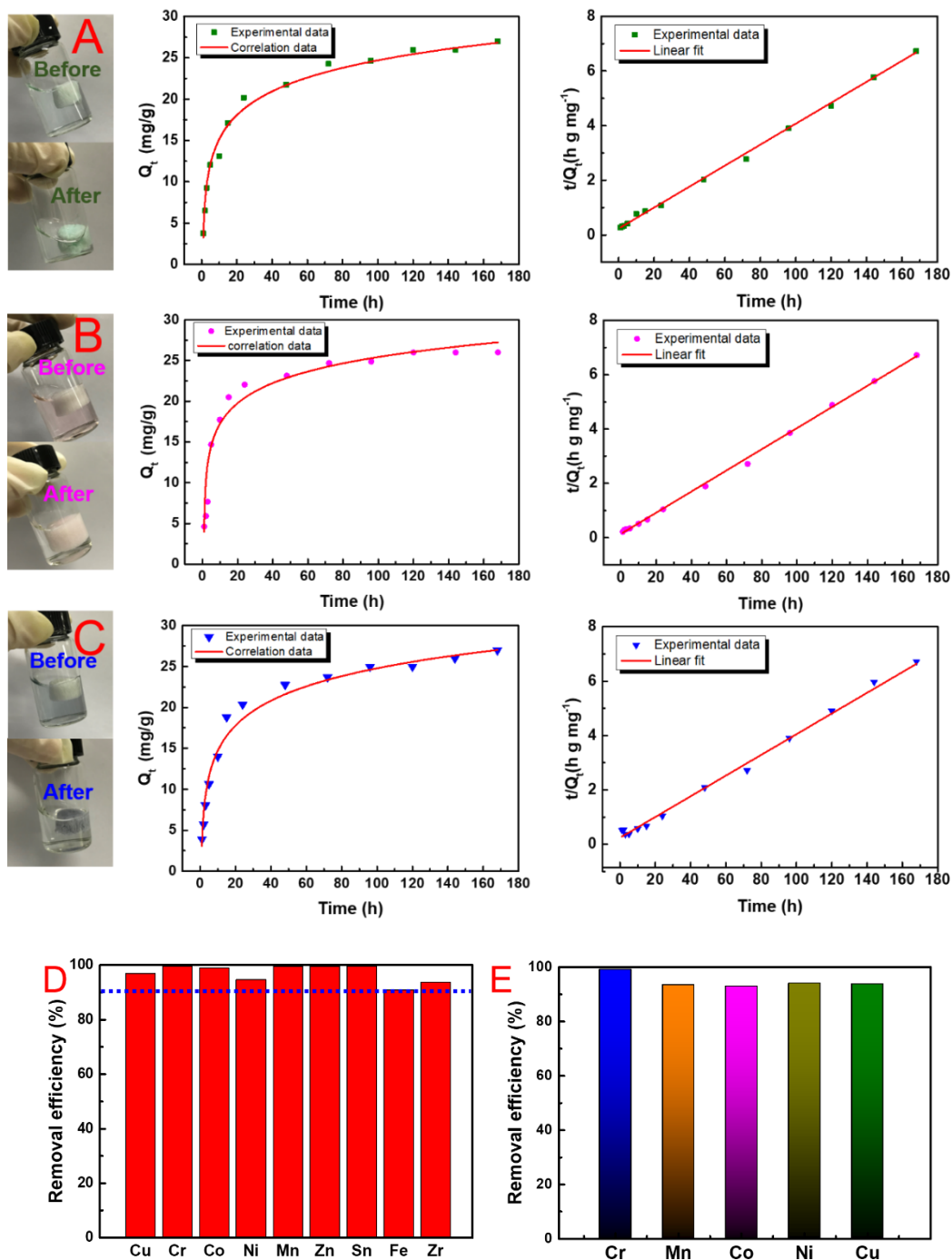


Figure 5: The time-dependent adsorption and pseudo-second-order plots. A, B, C)

The adsorption kinetics of adsorption of Cu^{2+} , Co^{2+} , Cr^{3+} via U-EDTACCA, respectively.

D) The removal efficiency of heavy metal ions for U-EDTACCA. E) A simultaneous

removal efficiency for Cr^{3+} , Mn^{2+} , Co^{2+} , Ni^{2+} and Cu^{2+} metal ions in batch adsorption.

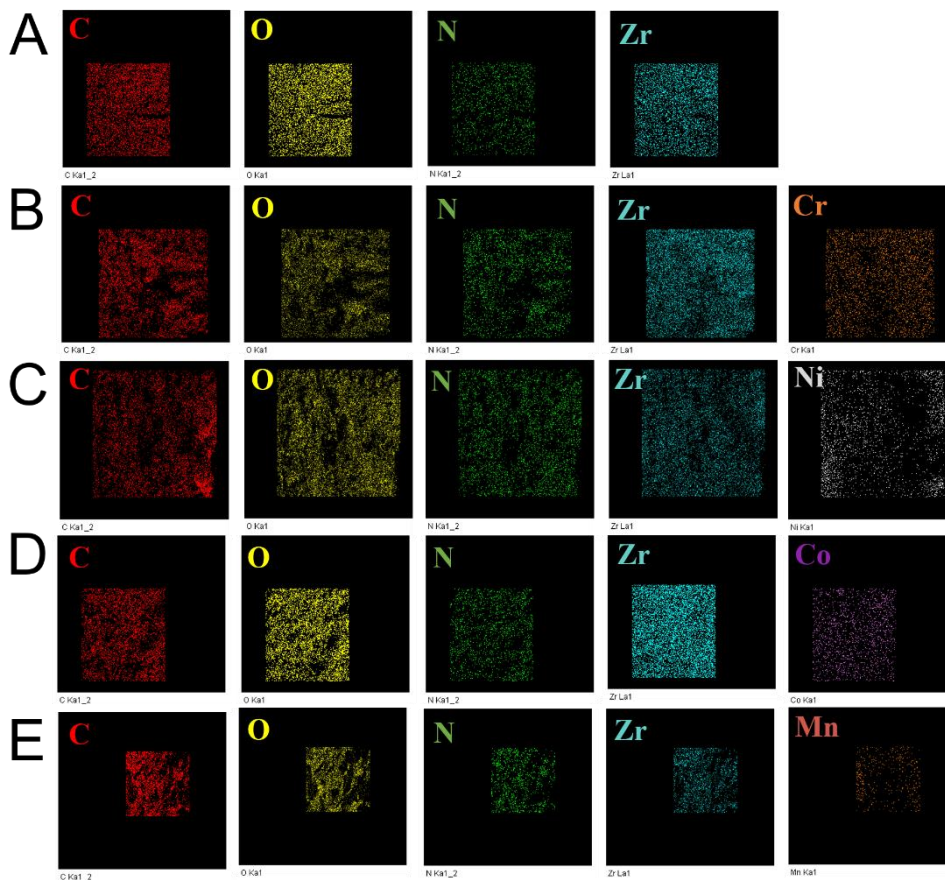


Figure 6: Dispersion state of metal ions in U-EDTA CCA . A) Corresponding elemental maps for U-EDTA CCA . B-E) single-metal system U-EDTA CCA loaded with Cr^{3+} , Ni^{2+} , Co^{2+} and Mn^{2+} , respectively.

Recycling of adsorbents

As it is known, reusability is quite significant for the practical application for a good adsorbent. Thus, reusability of the samples was tested for several times. In this paper, U-EDTA CCA loaded with Cr^{3+} could recover to its original shape after a casually mechanical squeezing process (Figure 7A-F). Obviously, the trans-mutative aerogel could recover most of its original shape when after removing the stress applied to the aerogels (Figure 7F), which demonstrated excellent mechanical properties. Noteworthy,

the U-EDTA₂CCA loaded with metal ions could be reused by washing with a high concentration of EDTA-2Na solution. Figure 7G-I showed that the color of the aerogel changed from white color to pink color after loaded with Co²⁺ ions- and returned to white color after washed with EDTA-2Na solution. This phenomenon demonstrated that the prepared aerogel could be recycled easily. The regenerated aerogels were further used as samples in the following metal ions removal experiments. The U-EDTA₂CCA retained over 88% of the adsorption capacity for all the measured metal ions after 5 cycles (Figure 8A). As shown in Figure 8B, U-EDTA₂CCA could be compressed to 70% of their original shape without mechanical failure and presented 86 KPa at 70% strain. The U-EDTA₂CCA showed good stability after recycling for 5 cycles without obviously reduction in performance.

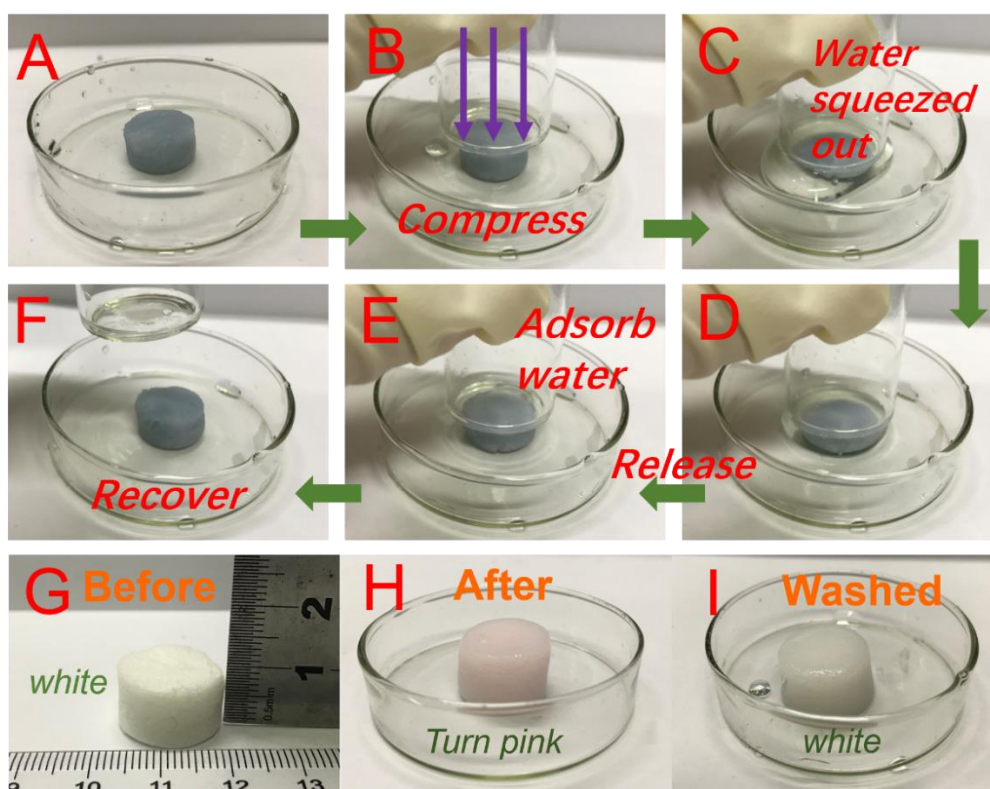


Figure 7: A-F) Images of U-EDTA₂CCA in the cyclic water absorption experiment.

G) Photographs of U-EDTA₂CCA. H) U-EDTA₂CCA loaded with Co²⁺. I) regenerated U-EDTA₂CCA.

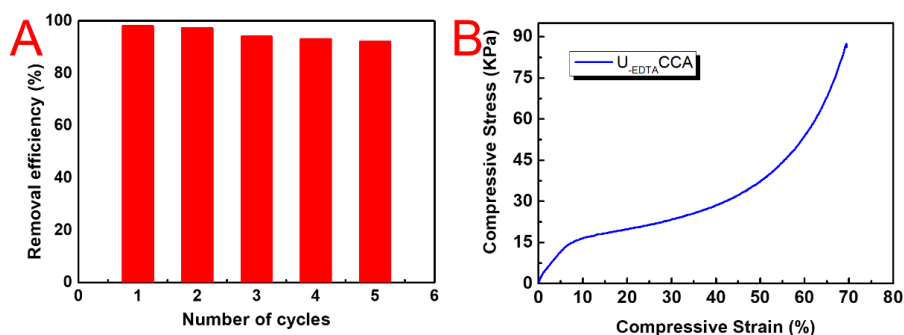


Figure 8: A) removal efficiency of Cr³⁺ by U-EDTA₂CCA after several cycles. B) Compressive stress-strain curves of U-EDTA₂CCA.

Conclusion

The flexible and high adsorptive adsorbent U-EDTA₂CCA was prepared by combining the functional UiO-66-EDTA and CNF into flexible aerogel followed by directional freeze-casting methods. The prepared aerogel exhibited outstanding shape stability and high removal efficiency. The adsorption experiment for total 9 kinds heavy metal ions showed that the removal efficiency was more than 91%. By controlling the concentration of CMC solution, aerogels produced three types pore structure with fibrillar, columnar, or lamellar morphologies. Apparently, this anisotropic pore structure was beneficial for improving the adsorption efficiency. The U-EDTA₂CCA showed excellent stability after recycling for 5 times without obviously reduction and the removal efficiencies was still over 88%. The U-EDTA₂CCA exhibited such good repeatability, reusability, and high adsorption properties which indicated that prepared aerogels were ideal material for removing heavy metal ions.

Materials and Methods

Materials

Douglas fir bleached pulp was bought from Zhongshan NFC Bio-Materials Co., Ltd. (GuangDong, China). ethylenediamine tetraacetic acid disodium salt (EDTA-2Na), sodium hypochlorite solution (NaClO), 2,2,6,6-tetramethylpyperidine-1-oxyl (TEMPO, 99.9%), cobalt (II) nitrate hexahydrate ($\text{Co}(\text{NO}_3)_2 \cdot 6\text{H}_2\text{O}$) and sodium bromide (NaBr, 99.6%) were purchased from Sigma Chemical Co. Zirconium (IV) chloride (98%). Chromium (III) nitrate nonahydrate ($\text{CrN}_3\text{O}_9 \cdot 9\text{H}_2\text{O}$), hydrochloric acid (HCl), copper sulfate pentahydrate ($\text{CuSO}_4 \cdot 5\text{H}_2\text{O}$), manganese acetate tetrahydrate ($\text{MnC}_4\text{H}_6\text{O}_4 \cdot 4\text{H}_2\text{O}$), Zinc nitrate hexahydrate ($\text{Zn}(\text{NO}_3)_2 \cdot 6\text{H}_2\text{O}$) and Ferric chloride hexahydrate ($\text{FeCl}_3 \cdot 6\text{H}_2\text{O}$) were achieved from Aladdin Industrial Corporation China. Carboxymethyl cellulose (CMC, M.W.250000, DS=0.7), sodium hydroxide (NaOH), N, N-dimethylformamide (DMF), terephthalic acid (BDC, 99%), nickel chloride hexahydrate ($\text{NiCl}_2 \cdot 6\text{H}_2\text{O}$), were achieved from Sinopharm Chemical Reagent Co. Ltd. Deionized water (resistivity: 18.25 M Ω /cm) was used to prepare aqueous solution.

The preparation of CNF suspension

The synthesis of CNF suspensions was accomplished according to the literature.[42] Douglas fir bleached pulp fibers (10 g) were added into DI water (1000 ml) and smashed with a grinder, then TEMPO (0.16 g) and NaBr (1 g) were further added into the suspension. Afterwards, NaClO (0.372 g) was added dropwise into the suspension with a vigorous stirring and the pH of the suspension was controlled at approximately 10 using NaOH solution (0.1 M). Lastly, the suspension of the fiber was passed through a high-pressure homogenizer after the chemical pretreatment to obtain the CNF suspension.

The preparation of UiO-66-EDTA

UiO-66 powder was prepared on the basis of the literature.[43] In brief, $ZrCl_4$ (1 g) and BDC (0.713 g) were dissolved in DMF (250 mL) at room temperature. The mixed solution was stirred using a vortex mixer and added acetic acid (10 mL) quickly at the same time, and then kept at 120 °C for 24 h. The prepared solid washed and collected by centrifuge. The resulting powder was dried under vacuum oven at 102 °C for further experiments. Then, activated UiO-66 powder (0.1 g) was added to EDTA solution (50 ml, 3.8 wt%) and kept at 60 °C for 24 h. Then, the product was further washed several times with DI water and then collected through filtration. Finally, the powders were obtained after drying at 60 °C overnight.

The preparation of anisotropic U-EDTA/CCA

The functional UiO-66-EDTA powder (0.1 g) was added into 1 wt% CNF (10 g) suspension for the purpose of sonication. Subsequently, different concentration of CMC (1 wt%, 2 wt%, 4 wt%) was added into the suspension (mass ratio CNF: CMC=1:1) and vigorously stirred for 1 h. The prepared mixed solution was putted in vacuum oven to remove small bubbles and then kept at 75 °C for 1 h for curing before transferred into freezing equipment. The obtained mixed solution was frozen using liquid nitrogen (−196 °C) via a self-made equipment shown in Figure 2.

Characterization

The concentration of metal ions aqueous solution was measured by an inductively coupled plasma-mass spectrometry NeXion 300X (ICP-MS, PE, USA). The morphology images of the obtained aerogels were conducted by JSM-7600F field

emission scanning electron microscope (FESEM, JEOL, Japan). The IR analysis of samples was carried out on a FTIR Bruker VERTEX 80 spectrometer (Bruker, Germany). The spectral range of IR experiment is 4000-600 cm^{-1} . The X-ray diffraction (XRD) analysis of materials were determined on Ultima IV X-ray diffractometer (Rigaku, Japan) with using a Cu $K\alpha$ radiation as a source. The XRD spectra were collected from $2\theta=5-60^\circ$. The X-ray photoelectron spectroscopy analysis of samples were measured by using an AXIS UltraDLD (Shimadzu, UK) with Al $K\alpha$ X-ray as the excitation source.

Heavy metal ions adsorption experiments

Solutions containing heavy metal ions were prepared through dissolving specific metal salt in deionized water. In this paper, Cr^{3+} , Cu^{2+} , Co^{2+} , Ni^{2+} , Mn^{2+} , Zn^{2+} , Sn^{4+} , Fe^{3+} and Zr^{4+} was chosen as target-ion mercury pollutant. U-EDTACCA (0.004 g) was poured into 10 ml water containing heavy metal ions and kept at room temperature for 120 hours to get the adsorption equilibrium. The pH of the metal ions solution was kept neutral and adjusted by 0.1 M HCl and 0.1 M NaOH. Afterwards, aerogels filled fully with metal ions was filtered through a membrane filter thoroughly for removing impurities. The concentration of the solution containing heavy metal ions after adsorption was measured by ICP-MS. The adsorption capacity Q_t (mg g^{-1}) of the absorbents and the removal percentage E were calculated using equations (1) and (2), respectively.

$$Q_t = \frac{(C_0 - C_t)}{M} \cdot V \quad (1)$$

$$E = \frac{(C_0 - C_e)}{C_0} \times 100\% \quad (2)$$

In the above equations, C_0 (mg L^{-1}) represents initial concentration, C_t (mg L^{-1}) means the concentration at time t , C_e (mg L^{-1}) equals to the equilibrium concentrations. M (g) means the weight of adsorbent and V (L) is the volume of heavy metal ions solutions.

The rate constant of adsorption was corresponded to the pseudo-first-order equation as follows equations (3) and (4):

$$\ln(Q_e - Q_t) = \ln Q_e - k_1 t \quad (3)$$

$$\frac{t}{Q_t} = \frac{1}{k_2 Q_e^2} + \frac{t}{Q_e} \quad (4)$$

In the above equation, Q_e (mg g^{-1}) represents the adsorption capacities at equilibrium, Q_t (mg g^{-1}) means the adsorption capacities at time t (h), k_1 means the rate constant of the pseudo-first-order model. The time-dependence of the adsorption is fitted with the pseudo-second-order kinetic model. k_2 is the rate constant of the pseudo-first-order model.

Acknowledgments

This work was supported by Key Laboratory of Bio-based Material Science & Technology (Northeast Forestry University), Ministry of Education (SWZ-ZD201906) and the National Natural Science Foundation of China (31770607). The authors acknowledge the Advanced Analysis & Testing Center of Nanjing Forestry University.

References

1. Fu, F.; Wang, Q. *Journal of Environmental Management* **2011**, *92*, 407–418.
2. Lam, K.F.; Chen, X.; McKay, G.; Yeung, K.L. *Ind. Eng. Chem. Res.* **2008**, *47*, 9376–9383.
3. Yuan, J.; Hung, W.-S.; Zhu, H.; Guan, K.; Ji, Y.; Mao, Y.; Liu, G.; Lee, K.-R.; Jin, W. *Journal of Membrane Science* **2019**, *572*, 20–27.
4. Ki, C.; Gang, E.; Um, I.; Park, Y. *Journal of Membrane Science* **2007**, *302*, 20–26.
5. d'Halluin, M.; Rull-Barrull, J.; Bretel, G.; Labrugère, C.; Le Grogneec, E.; Felpin, F.-X. *ACS Sustainable Chem. Eng.* **2017**, *5*, 1965–1973.
6. Peterson, E.A.; Sober, H.A. *J. Am. Chem. Soc.* **1956**, *78*, 751–755.
7. Chen, G. *Separation and Purification Technology* **2004**, *38*, 11–41.
8. Lin, S.H.; Lin, C.M. *Water Research* **1993**, *27*, 1743–1748.
9. Xu, Q.; Wang, Y.; Jin, L.; Wang, Y.; Qin, M. *Journal of Hazardous Materials* **2017**, *339*, 91–99.
10. He, X.; Cheng, L.; Wang, Y.; Zhao, J.; Zhang, W.; Lu, C. *Carbohydrate Polymers* **2014**, *111*, 683–687.
11. Yamaguchi, H.; Higasida, R.; Higuchi, M.; Sakata, I. *Journal of Applied Polymer Science* **1992**, *45*, 1463–1472.
12. Saliba, R.; Gauthier, H.; Gauthier, R. *Adsorption Science & Technology* **2005**, *23*, 313–322.
13. Lv, X.; Zhao, M.; Chen, Z.; Zhang, J.; Tian, X.; Ren, X.; Mei, X. *Colloid and*

- Polymer Science* **2018**, *296*, 59–70.
14. El-Khouly, A.S.; Takahashi, Y.; Saafan, A.A.; Kenawy, E.; Hafiz, Y.A. *Journal of Applied Polymer Science* **2011**, *120*, 866–873.
 15. Wan, W.; Zhang, R.; Ma, M.; Zhou, Y. *Journal of Materials Chemistry A* **2017**.
 16. Zheng, Q.; Javadi, A.; Sabo, R.; Cai, Z.; Gong, S. *RSC Advances* **2013**, *3*, 20816.
 17. Zhu, L.; Zong, L.; Wu, X.; Li, M.; Wang, H.; You, J.; Li, C. *ACS Nano* **2018**, *12*, 4462–4468.
 18. Zheng, Q.; Cai, Z.; Ma, Z.; Gong, S. *ACS Applied Materials & Interfaces* **2015**, *7*, 3263–3271.
 19. Tan, S.; Li, J.; Zhou, L.; Chen, P.; Xu, D.; Xu, Z. *Journal of Materials Science* **2018**, *53*, 11648–11658.
 20. Wu, Z.-Y.; Liang, H.-W.; Chen, L.-F.; Hu, B.-C.; Yu, S.-H. *Accounts of Chemical Research* **2016**, *49*, 96–105.
 21. Wu, B.; Zhu, G.; Dufresne, A.; Lin, N. *ACS Appl. Mater. Interfaces* **2019**, *11*, 16048–16058.
 22. Köhnke, T.; Lin, A.; Elder, T.; Theliander, H.; Ragauskas, A.J. **2012**, *6*.
 23. Li, T.; Song, J.; Zhao, X.; Yang, Z.; Pastel, G.; Xu, S.; Jia, C.; Dai, J.; Chen, C.; Gong, A.; et al. *Science Advances* **2018**, *4*, eaar3724.
 24. Wang, D.; Yu, H.; Fan, X.; Gu, J.; Ye, S.; Yao, J.; Ni, Q. *ACS Applied Materials & Interfaces* **2018**, *10*, 20755–20766.
 25. Yang, X.; Bakaic, E.; Hoare, T.; Cranston, E.D. *Biomacromolecules* **2013**, *14*, 4447–4455.

26. Li, Y.; Liu, Y.; Liu, Y.; Lai, W.; Huang, F.; Ou, A.; Qin, R.; Liu, X.; Wang, X. *ACS Sustainable Chemistry & Engineering* **2018**.
27. Chau, M.; Reyes, L.; Chan, K.J.W.; Fo, S.; Kumacheva, E. *Chem. Mater.* **2016**, 10.
28. Xu, Z.; Jiang, X.; Zhou, H.; Li, J. *Cellulose* **2018**, 25, 1217–1227.
29. Zhang, W.; Lu, G.; Cui, C.; Liu, Y.; Li, S.; Yan, W.; Xing, C.; Chi, Y.R.; Yang, Y.; Huo, F. *Advanced Materials* **2014**, 26, 4056–4060.
30. Howarth, A.J.; Liu, Y.; Li, P.; Li, Z.; Wang, T.C.; Hupp, J.T.; Farha, O.K. *Nature Reviews Materials* **2016**, 1.
31. Denny, M.S.; Moreton, J.C.; Benz, L.; Cohen, S.M. *Nature Reviews Materials* **2016**, 1, 16078.
32. Van de Voorde, B.; Bueken, B.; Denayer, J.; De Vos, D. *Chem. Soc. Rev.* **2014**, 43, 5766–5788.
33. Yang, Q.; Wang, Y.; Wang, J.; Liu, F.; Hu, N.; Pei, H.; Yang, W.; Li, Z.; Suo, Y.; Wang, J. *Food Chemistry* **2018**, 254, 241–248.
34. Peng, Y.; Huang, H.; Zhang, Y.; Kang, C.; Chen, S.; Song, L.; Liu, D.; Zhong, C. *Nature Communications* **2018**, 9.
35. Zhu, H.; Yang, X.; Cranston, E.D.; Zhu, S. *Advanced Materials* **2016**, 28, 7652–7657.
36. Rangnekar, N.; Mittal, N.; Elyassi, B.; Caro, J.; Tsapatsis, M. *Chem. Soc. Rev.* **2015**, 44, 7128–7154.
37. Lei, C.; Gao, J.; Ren, W.; Xie, Y.; Abdalkarim, S.Y.H.; Wang, S.; Ni, Q.; Yao, J.

- Carbohydrate Polymers* **2019**, *205*, 35–41.
38. Astrini, N.; Anah, L.; Haryadi, H.R. *Macromolecular Symposia* **2015**, *353*, 191–197.
 39. Liu, P.; Borrell, P.F.; Božič, M.; Kokol, V.; Oksman, K.; Mathew, A.P. *Journal of Hazardous Materials* **2015**, *294*, 177–185.
 40. Wang, J.; Liu, M.; Duan, C.; Sun, J.; Xu, Y. *Carbohydrate Polymers* **2019**, *206*, 837–843.
 41. Omri, A.; Benzina, M. *Alexandria Engineering Journal* **2012**, *51*, 343–350.
 42. Isogai, A.; Saito, T.; Fukuzumi, H. *Nanoscale* **2011**, *3*, 71–85.
 43. Kandiah, M.; Nilsen, M.H.; Usseglio, S.; Jakobsen, S.; Olsbye, U.; Tilset, M.; Larabi, C.; Quadrelli, E.A.; Bonino, F.; Lillerud, K.P. *Chemistry of Materials* **2010**, *22*, 6632–6640.